Supplement of The Cryosphere, 18, 1381–1398, 2024
https://doi.org/10.5194/tc-18-1381-2024-supplement

The Cryosphere Open Access EGU

Supplement of

Modeling the timing of Patagonian Ice Sheet retreat in the Chilean Lake District from 22–10 ka

Joshua Cuzzone et al.

Correspondence to: Joshua Cuzzone (joshua.k.cuzzone@jpl.nasa.gov)

Section 1

LGM Steady State Ice Temperature

In order to test the validity of our assumption of a largely temperate based ice sheet across this domain, we calculate ice temperature at the LGM, assuming the ice sheet is in a steady-state thermal equilibrium following Serrousi et al. (2013). This methodology has been used for numerous applications in Greenland and Antarctica to calculate the thermal conditions of the ice sheets (Seroussi et al., 2013; MacGregor et al., 2016; Goelzer et al., 2020; Seroussi et al., 2020). We use our modeled LGM ice sheet geometry from this analysis to calculate the thermal conditions of the ice sheet. This formulation, outlined in Seroussi et al. (2013) uses an enthalpy formulation from Aschwanden et al. (2012) that includes both temperate and cold ice. LGM air temperature is imposed at the surface and geothermal heat flux is applied at the base (100 mW m−2 mean from Hamza and Vieira, 2018). For this step, we extrude our 2D model to 3D, with the model for the thermal state calculation having 20 layers.

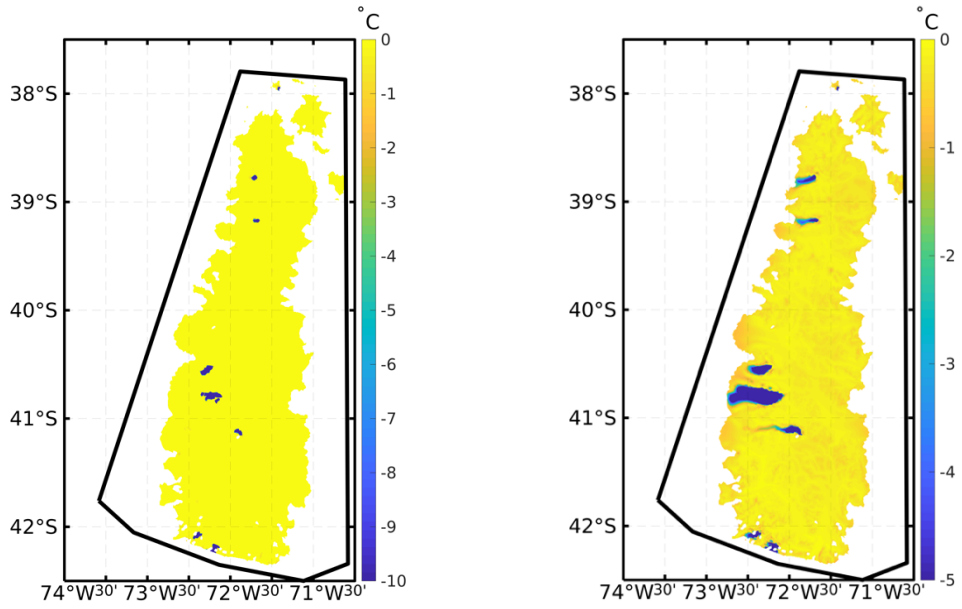

Figure S1. Simulated Steady State LGM basal pressure adjusted temperature in degrees Celsius (left panel). Simulated depth averaged ice temperature in degrees Celsius (right panel).

Here we show the simulated Steady State Basal Temperatures (Figure S1 left panel) and the simulated Depth Averaged Steady State temperatures (Figure S1 right panel). The ice sheet is mainly warm based (figure A) with temperatures near 0 degrees Celsius, with exception for some of the high peaks where ice cover is thin enough for the colder surface temperatures to diffuse and advect downward. The depth averaged temperature (figure S1 right panel) shows that the majority of the ice sheet is between -1 to 0 degrees Celsius, with the mean of the depth averaged temperature being -0.41 degrees Celsius. There are some exceptions, where colder ice seems to be advected downstream from the colder based high peaks (in figure S1 left panel), however, we must note that these simulated temperatures are likely an underestimate as they do not account fully for frictional heating that would occur If the 3D thermal model was run transiently to steady state. Therefore,

this analysis provides some level of confidence in our assumption of a temperate ice sheet across the CLD.

Section 2

Prescribed GIA forcing

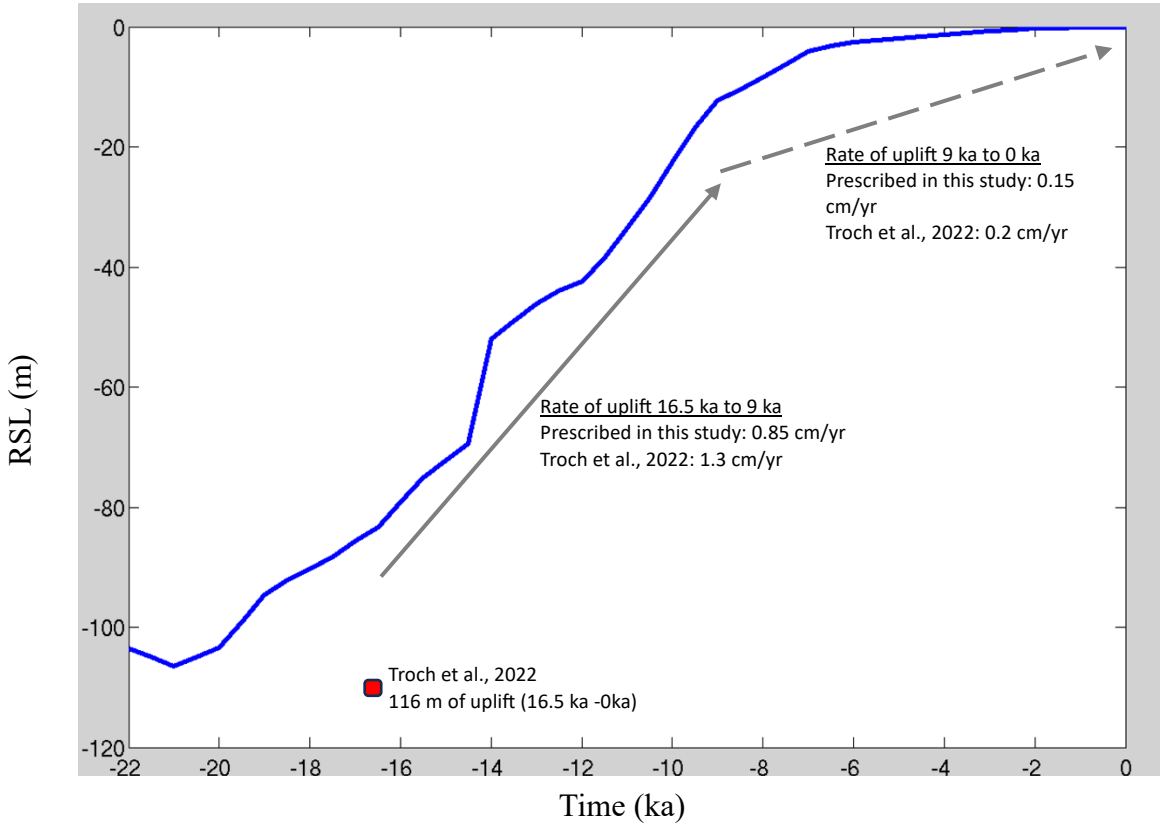

Figure S2: The time dependent prescribed relative sea level change area averaged across our model domain. The relative sea-level change consists of 1) Bedrock vertical motion, 2.) Eustatic sea level change, and 3.) Geoid changes from Caron et al., 2018 across the last deglaciation. For reference, we show the reconstructed total uplift from and isolation basin in Central Patagonia (Troch et al., 2022; 116m between 16.5 ka and 0 ka), and the associated uplift rates compared against our study (16.5 ka to 9 ka; 9ka to 0 ka).

Section 3

Wintertime (JJA) 925 hPA zonal wind

Figure S3 A-E. First column: The difference in the JJA 925 hPa zonal wind for each corresponding time period relative to the PI (in m/s). Positive values indicate increased zonal wind speed and negative values indicate decreased zonal wind speed relative to the PI. The magenta line is the position of the maximum zonal wind during the PI. The black line is the position of the maximum zonal wind for the corresponding time period. The red polygon denotes the location of our model domain. Second column: Zonal mean JJA 925 hPa wind (in m/s) averaged over -85 to -55 degrees west longitude for the PI and the corresponding time period. Time periods listed are computed over 500 yr periods (***LGM***: 22ka-21.5ka; ***18ka***: 18.5ka-18ka; ***16ka***: 16.5ka-16ka; ***14ka***: 14.5ka-14ka; ***12ka***: 12.5ka-12ka).

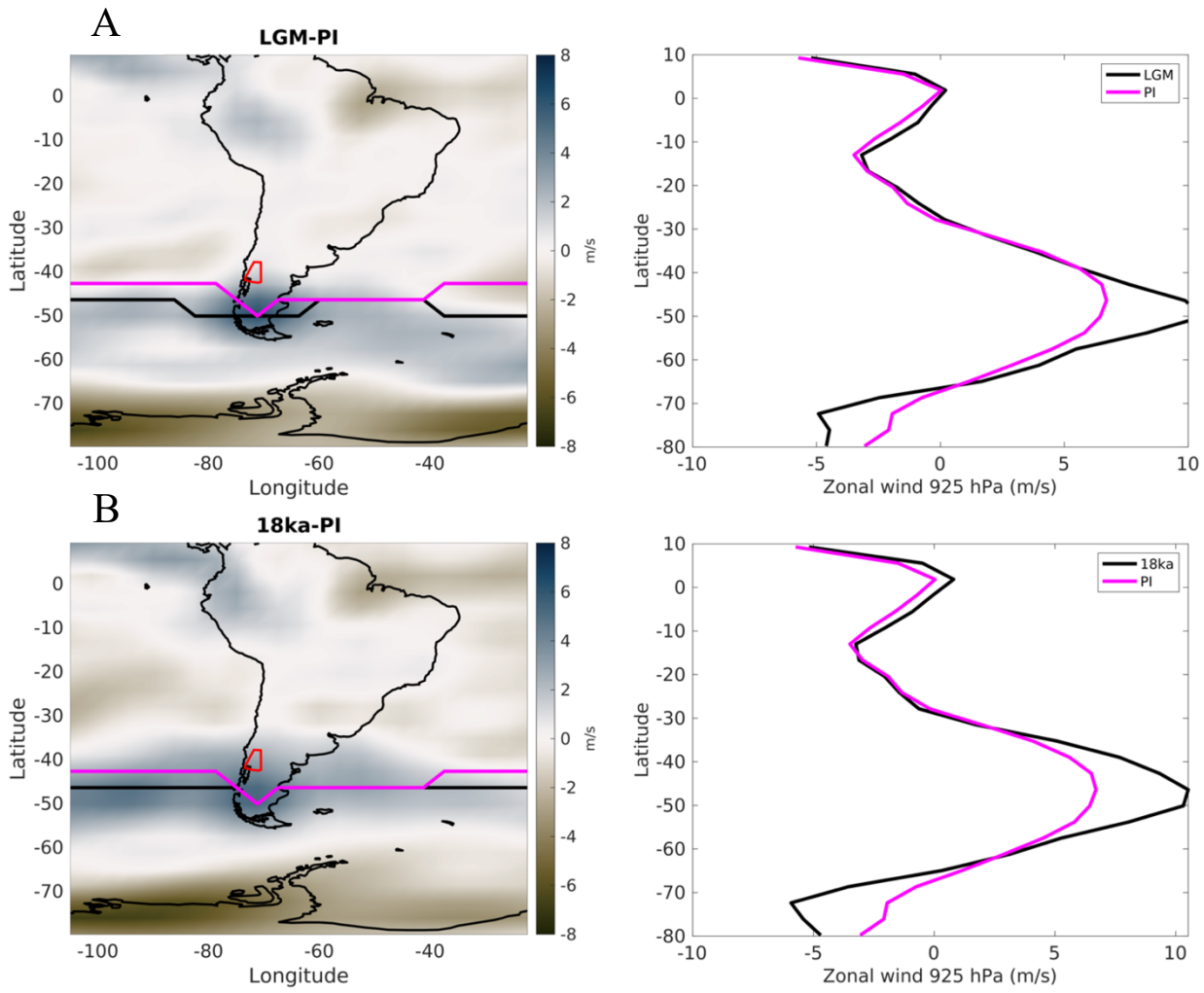

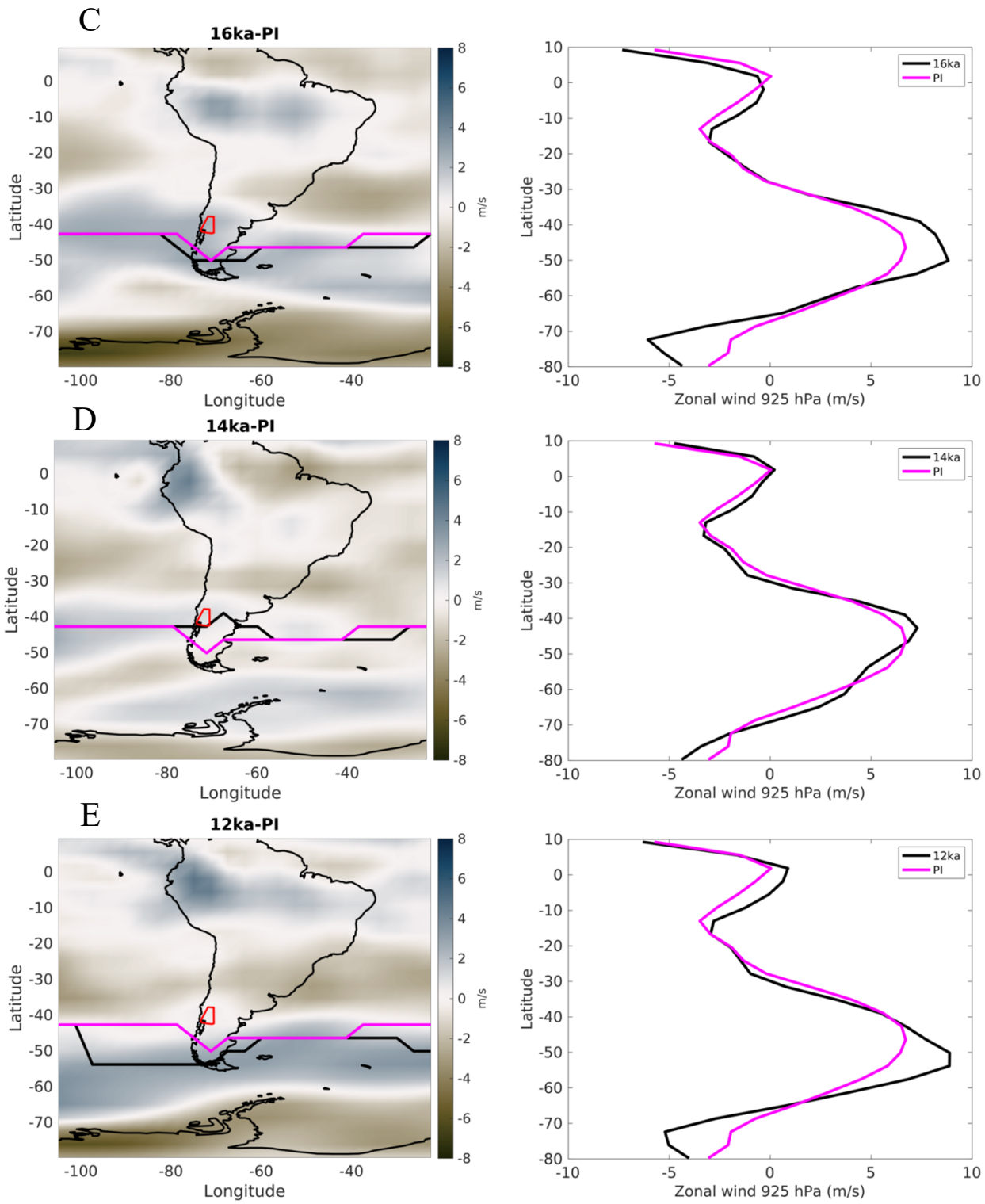

144
145
146
147
148
149
150

850 hPa Moisture Flux Convergence

We calculate the moisture flux convergence (MFC) at 850 hPa as:

$$-1(\nabla \cdot Vq)$$

where ∇ is the gradient operator, V is the horizontal wind vector (u,v), and q is the specific humidity. The divergence is multiplied in this case by -1 to show moisture flux convergence. We calculate the MFC at the ***LGM*** (22ka-21.5ka), ***18ka*** (18.5ka-18ka), ***16ka*** (16.5ka-16ka), ***14ka*** (14.5ka-14ka), and ***12ka*** (12.5ka-12ka) and then compute the difference at these periods against the **PI** (shown below in Figure S4A-E).

Figure S4 A-E. JJA moisture flux convergence at 850 hPA for each corresponding time period, computed as the difference from the PI (in g $kg^{-1}s^{-1}$). Positive anomalies indicate areas of greater moisture flux convergence relative to the PI and negative values indicate areas of greater moisture flux divergence relative to the PI. The wind vectors correspond to the anomaly relative to the PI for the 850 hPa. The red polygon denotes the location of our model domain. Time periods listed are computed over 500 yr periods (***LGM***: 22ka-21.5ka; ***18ka***: 18.5ka-18ka; ***16ka***: 16.5ka-16ka; ***14ka***: 14.5ka-14ka; ***12ka***: 12.5ka-12ka).

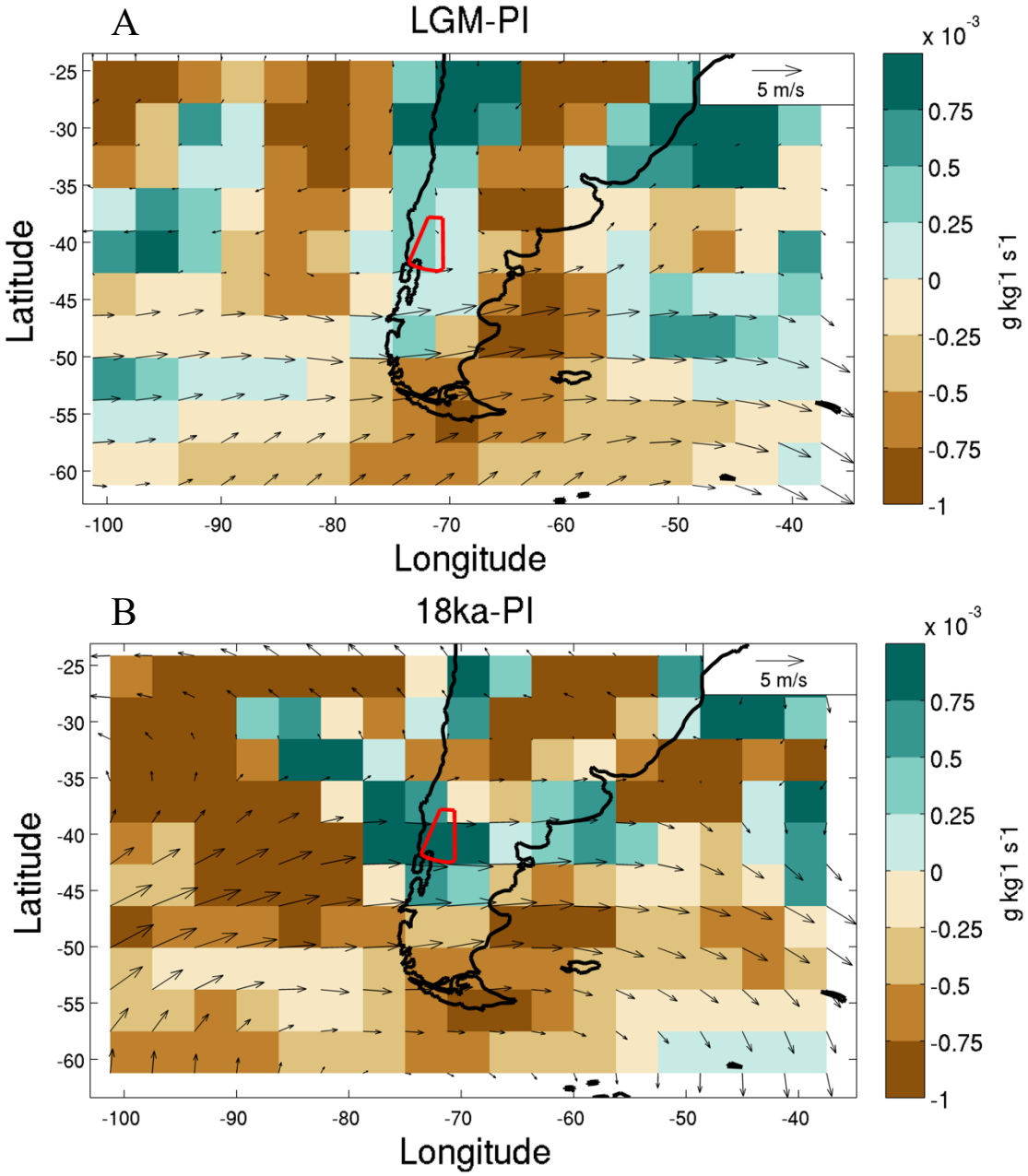

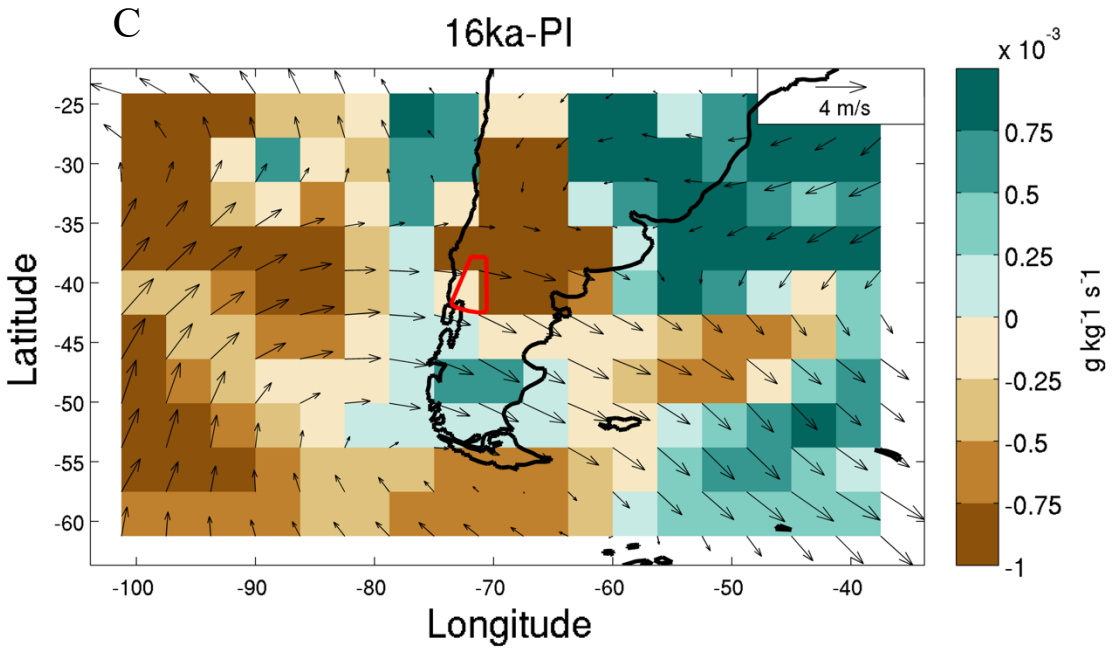
C
16ka-PI
4 m/s
x 10^-3
0.75
0.5
0.25
0
-0.25
-0.5
-0.75
-1
g kg^-1 s^-1
Latitude
Longitude
-25
-30
-35
-40
-45
-50
-55
-60
-100
-90
-80
-70
-60
-50
-40

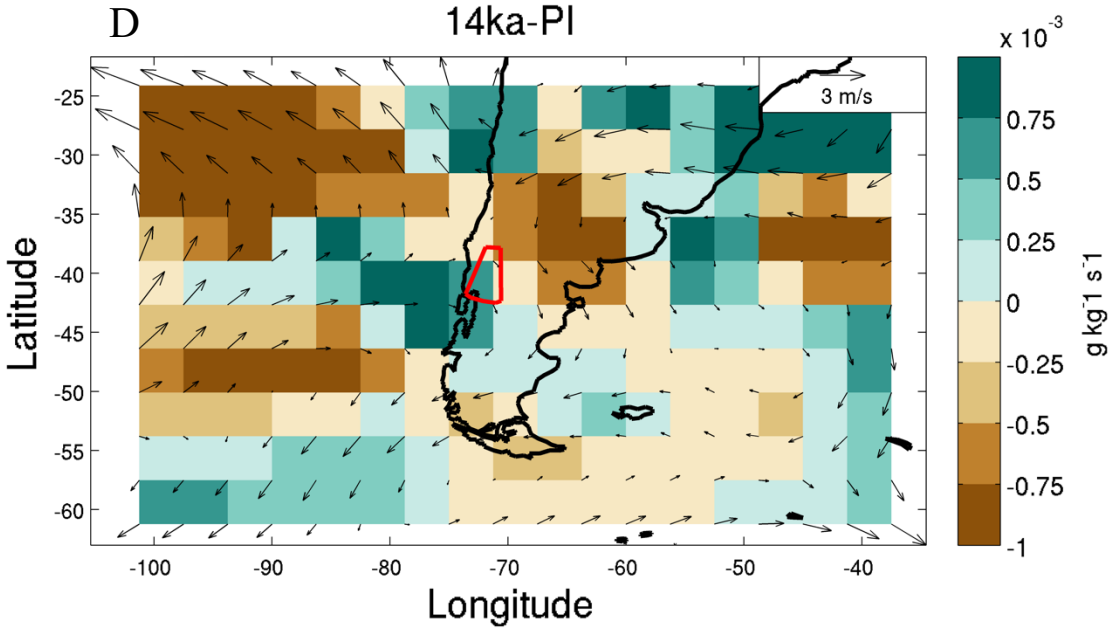
D
14ka-PI
3 m/s
x 10^-3
0.75
0.5
0.25
0
-0.25
-0.5
-0.75
-1
g kg^-1 s^-1
Latitude
Longitude
-25
-30
-35
-40
-45
-50
-55
-60
-100
-90
-80
-70
-60
-50
-40

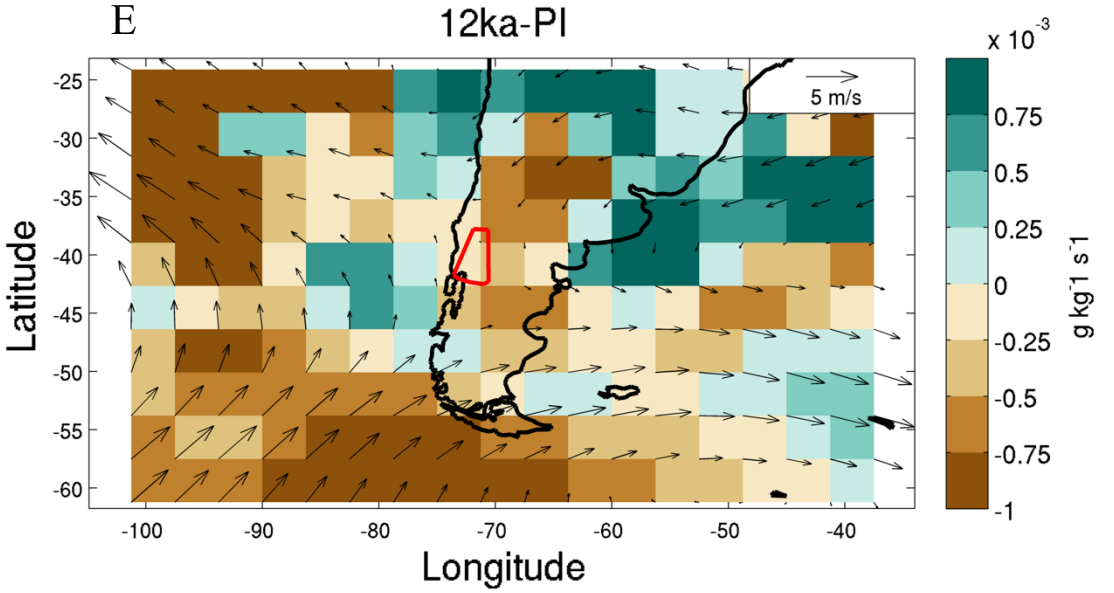
E
12ka-PI
5 m/s
x 10^-3
0.75
0.5
0.25
0
-0.25
-0.5
-0.75
-1
g kg^-1 s^-1
Latitude
Longitude
-25
-30
-35
-40
-45
-50
-55
-60
-100
-90
-80
-70
-60
-50
-40

206

References

Aschwanden, A., Bueler, E., Khroulev, C., and Blatter, H.: An enthalpy formulation for glaciers and ice sheets, J. Glaciol., 58, 441–457, https://doi.org/10.3189/2012JoG11J088, 2012.

Darvill, C.M., Stokes, C.R., Bentley, M.J., Evans, D.J.A., Lovell, H. Dynamics of former ice lobes of the southernmost Patagonian Ice Sheet based on a glacial landsystems approach. Journal of Quaternary Science. 32,6,857-876. https://doi.org/10.1002/jqs.2890

Goelzer, H., Nowicki, S., Payne, A., Larour, E., Seroussi, H., Lipscomb, W. H., Gregory, J., Abe-Ouchi, A., Shepherd, A., Simon, E., Agosta, C., Alexander, P., Aschwanden, A., Barthel, A., Calov, R., Chambers, C., Choi, Y., Cuzzone, J., Dumas, C., Edwards, T., Felikson, D., Fettweis, X., Golledge, N. R., Greve, R., Humbert, A., Huybrechts, P., Le clec'h, S., Lee, V., Leguy, G., Little, C., Lowry, D. P., Morlighem, M., Nias, I., Quiquet, A., Rückamp, M., Schlegel, N.-J., Slater, D. A., Smith, R. S., Straneo, F., Tarasov, L., van de Wal, R., and van den Broeke, M.: The future sea-level contribution of the Greenland ice sheet: a multi-model ensemble study of ISMIP6, The Cryosphere, 14, 3071–3096, https://doi.org/10.5194/tc-14-3071-2020, 2020.

Hamza, V. M. and Vieira, F.: Global heat flow: new estimates using digital maps and GIS techniques, International Journal of Terrestrial Heat 490 Flow and Applied Geothermics, 1, 6–13, https://doi.org/10.31214/ijthfa.v1i1.6, 2018

MacGregor, J. A., Fahnestock, M. A., Catania, G. A., Aschwanden, A., Clow, G. D., Colgan, W. T., Gogineni, S. P., Morlighem, M., Nowicki, S. M., Paden, J. D., and Price, S. F.: A synthesis of the basal thermal state of the Greenland Ice Sheet, J. Geophys. Res.-Earth, 121, 1328–1350, 2016.

Seroussi, H., Nowicki, S., Payne, A. J., Goelzer, H., Lipscomb, W. H., Abe-Ouchi, A., Agosta, C., Albrecht, T., Asay-Davis, X., Barthel, A., Calov, R., Cullather, R., Dumas, C., Galton-Fenzi, B. K., Gladstone, R., Golledge, N. R., Gregory, J. M., Greve, R., Hattermann, T., Hoffman, M. J., Humbert, A., Huybrechts, P., Jourdain, N. C., Kleiner, T., Larour, E., Leguy, G. R., Lowry, D. P., Little, C. M., Morlighem, M., Pattyn, F., Pelle, T., Price, S. F., Quiquet, A., Reese, R., Schlegel, N.-J., Shepherd, A., Simon, E., Smith, R. S., Straneo, F., Sun, S., Trusel, L. D., Van Breedam, J., van de Wal, R. S. W., Winkelmann, R., Zhao, C., Zhang, T., and Zwinger, T.: ISMIP6 Antarctica: a multi-model ensemble of the Antarctic ice sheet evolution over the 21st century, The Cryosphere, 14, 3033–3070, https://doi.org/10.5194/tc-14-3033-2020, 2020.

Seroussi, H., Morlighem, M., Rignot, E., Khazendar, A., Larour, E., & Mouginot, J. (2013). Dependence of century-scale projections of the Greenland ice sheet on its thermal regime. Journal of Glaciology, 59(218), 1024–1034. https://doi.org/10.3189/2013JoG13J054